Surface-Bound Casein Modulates the Adsorption and Activity of Kinesin on SiO_2 Surfaces

Tomomitsu Ozeki,[†‡] Vivek Verma,[§] Maruti Uppalapati,[‡] Yukiko Suzuki,[†] Mikihiko Nakamura,[†] Jeffrey M. Catchmark,[¶] and William O. Hancock[‡*]

[†]ULVAC Inc., Kanagawa 253-8543, Japan; and [‡]Department of Bioengineering, [§]Department of Engineering Science and Mechanics, and [¶]Department of Agricultural and Biological Engineering, Penn State University, University Park, Pennsylvania 16802

ABSTRACT Conventional kinesin is routinely adsorbed to hydrophilic surfaces such as SiO_2. Pretreatment of surfaces with casein has become the standard protocol for achieving optimal kinesin activity, but the mechanism by which casein enhances kinesin surface adsorption and function is poorly understood. We used quartz crystal microbalance measurements and microtubule gliding assays to uncover the role that casein plays in enhancing the activity of surface-adsorbed kinesin. On SiO_2 surfaces, casein adsorbs as both a tightly bound monolayer and a reversibly bound second layer that has a dissociation constant of 500 nM and can be desorbed by washing with casein-free buffer. Experiments using truncated kinesins demonstrate that in the presence of soluble casein, kinesin tails bind well to the surface, whereas kinesin head binding is blocked. Removing soluble casein reverses these binding profiles. Surprisingly, reversibly bound casein plays only a moderate role during kinesin adsorption, but it significantly enhances kinesin activity when surface-adsorbed motors are interacting with microtubules. These results point to a model in which a dynamic casein bilayer prevents reversible association of the heads with the surface and enhances association of the kinesin tail with the surface. Understanding protein-surface interactions in this model system should provide a framework for engineering surfaces for functional adsorption of other motor proteins and surface-active enzymes.

INTRODUCTION

Many in vitro assays require binding proteins tightly to surfaces such as glass, plastic, gold, and silica while retaining proper function of the adsorbed proteins. For instance, antibodies are routinely adsorbed to surfaces and used to bind other proteins of interest, and avidin can be bound nonspecifically to surfaces and used to bind biotinylated proteins or DNA. However, despite the importance of such protein immobilization techniques in fundamental and applied research, there is little systematic understanding of these processes, and in most cases optimal utility is achieved only by trial and error.

In vitro motility assays, in which motor proteins such as kinesin, myosin, or dynein are adsorbed to glass surfaces or beads have provided a wealth of information regarding the fundamental mechanism of mechanoenzymes and have provided a model for incorporating biologically derived forces and transport into engineered microdevices (1–5). Approaches for attaching motor proteins to surfaces have included binding them to immobilized antibodies or streptavidin (6,7), pretreating surfaces with nitrocellulose (8), and adsorbing motors directly to the surface after pretreatment with a blocking protein (3,9). Despite the body of biophysical data generated from these assays, there is no systematic approach for immobilizing motor proteins (or other proteins for that matter) on surfaces. For instance, Månsson et al. have proposed a model for myosin in which the positively charged head domain binds to negatively charged surfaces such as glass and inactivates, whereas the C-terminal coiled-coil binds well to hydrophobic surfaces (10,11). This model explains the finding that heavy meromyosin is very active on hydrophobic surfaces but minimally active on clean glass, but as kinesin shows maximal activity on glass surfaces and is inactive when adsorbed to hydrophobic surfaces (12), this model is clearly not generalizable. Because there are dozens of motor proteins that have yet to be analyzed, and because better immobilization and precise patterning of motors could lead both to more precise functional assays and novel applications of motor-driven transport in microscale geometries, a more thorough understanding of how motor proteins bind to surfaces is needed.

Kinesin motors use the energy of ATP hydrolysis to transport intracellular cargo along microtubules, 25-nm-diameter cytoskeletal filaments. Conventional kinesin is a dimeric protein consisting of three domains: the heads, which bind microtubules and hydrolyze ATP, the coiled-coil rod, and the tail, which is responsible for cargo binding (13,14). In the microtubule gliding assay, which was instrumental in the discovery of conventional kinesin (15,16), motors are adsorbed to the surface through their tail domains, while the heads bind to and transport microtubules across the surface. Howard et al. showed that although adsorbing high concentrations of purified motors to glass resulted in functional immobilized motors, motor functionality on the surface was significantly enhanced by pretreating the surface with blocking proteins (3), and subsequent work showed that maximal motor activity is achieved when surfaces are pretreated with

Submitted August 8, 2008, and accepted for publication December 18, 2008.

*Correspondence: wohbio@engr.psu.edu

Editor: Hideo Higuchi.

0006-3495/09/04/3305/14 $2.00

doi: 10.1016/j.bpj.2008.12.3960

the milk protein casein (17–19). Despite a paucity of supporting data, the working model is that casein binds to the surface in such a way that, when motors are introduced, the kinesin tail is able to bind to the surface between aggregates of adsorbed casein, but the adsorbed casein blocks binding of the kinesin head, maximizing motor functionality.

Although this model is consistent with casein's ability to enhance kinesin functionality, it leaves a number of unresolved questions. First, what is the structure of surface-adsorbed casein? Casein aggregates into complexes that range from a few nanometers to hundreds of nanometers in diameter (20,21), and surface binding may also alter casein structure. Second, how does casein enable kinesin tail binding while preventing binding of the head domains to the surface? A corollary of this is: does the kinesin tail bind directly to the surface, or does it bind to surface-adsorbed casein? A final question is, after the initial adsorption of casein to a clean surface, what is the role of casein in solution? Kerssemakers et al. (22) recently reported that microtubules in the gliding assay are on average 17 nm above the glass surface, which puts an upper limit on the size of surface-adsorbed casein whether the kinesin tails are adsorbed to the glass surface or to the surface-adsorbed casein. In another recent report, Verma et al. showed that, regardless of the conditions during kinesin adsorption to the surface, soluble casein added to the microtubule solution improves the activity of surface-adsorbed kinesin (23).

Casein is a versatile protein that gives milk both its white color and unique ''mouth feel'' as well as being a carrier of calcium. Whole casein is predominantly made up of four subunits (α_{S1}, α_{S2}, β, and κ) that range from 19 to 25 kDa (24). In the presence of calcium, casein forms micelles in the range of 50–500 nm (21,25,26), whereas in the absence of calcium the micelles disassemble into smaller assemblies, often called submicelles (20,21). Casein subunits are amphipathic (24), and it has been suggested that casein acts as a stabilizer of protein structure, or even as a chaperone in promoting proper protein folding (27–29). The critical micelle concentration (CMC) of β-casein has been reported in the range of 0.05% w/v (0.5 mg/mL), although it varies with temperature, ionic strength, and subunit content (30). A number of studies have investigated both the interactions between casein subunits and the interaction of casein with surfaces. By use of surface plasmon resonance, it was shown that the association between the various casein subunits varies with phosphorylation state, pH, and ionic strength (31). Using neutron scattering to measure casein binding to hydrophobic surfaces, Fragneto found that a monolayer of β-casein binds tightly, followed by a second loosely bound layer (32). Tiberg et al. found similar subunit interactions for casein adsorbed to silicon oxide and argued that these interactions are correlates of the intersubunit interactions that stabilize casein micelle structure (33).

Here we use quartz crystal microbalance (QCM) mass measurements and functional kinesin assays to investigate binding of casein and kinesin to SiO_2 surfaces. By measuring the linear change in the resonance frequency of the crystal with increasing mass, the QCM can detect binding of proteins and other analytes to surfaces down to nanogram levels (34,35). Motility assays complement these measurements by quantifying the surface density of functional adsorbed kinesin motors. We find that casein binds tightly to surfaces, with the amount of tightly bound casein equivalent to a 2.1-nm-thick protein monolayer. In addition to this irreversibly bound casein layer, a second, reversibly bound layer of casein adsorbs with a maximum mass of one-third of the tightly bound layer. This reversible ''weakly bound layer'' has a profound effect on motor binding and motor function.

METHODS

Casein, kinesin motors, and microtubules

Casein protein (C7078, Sigma, St. Louis, MO) was dissolved in BRB80 buffer (80 mM PIPES, 1 mM $MgCl_2$, and 1 mM EGTA, pH 6.9) overnight, centrifuged at 245,000 $\times$ g in a Beckman 50.2 Ti rotor for 30 min, and filtered through 0.22-μm syringe filters (Fisher Scientific) to remove insoluble components. Protein concentration was determined by absorbance at 280 nm, the protein was diluted to 20 mg/mL in BRB80, aliquoted, frozen at -20°C, and thawed the day of the experiment. Because the tertiary structure of casein is presumably dynamic and is not determined, casein binding data are presented as the molar concentration of casein subunits, where 24 kDa is taken as the average subunit molecular mass (i.e., 1 mg/mL = 44 μM subunits).

Full-length *Drosophila melanogaster* conventional kinesin heavy chain was bacterially expressed and purified by Ni column chromatography as previously described (2,36). A headless construct was generated by deleting the first 345 amino acids of *Drosophila* kinesin (2), and a tailless kinesin was constructed by truncating following M^{559} (37). Motor concentrations were estimated by gel densitometry using a UVP GelDoc system after staining with Coomassie blue or Sypro Orange (Molecular Probes, Carlsbad, CA).

Bovine brain tubulin was purified and rhodamine labeled as previously described (38,39). Microtubules were polymerized by combining 32 μM tubulin (1 rhodamine label per four tubulin dimers), 1 mM GTP, 4 mM $MgCl_2$, and 5% DMSO in BRB80 buffer and incubating at 37°C for 20 min, and were stabilized by diluting 100-fold into BRB80 including 10 μM taxol, which results in a population of microtubules with lengths in the range of 5–20 μm.

In vitro motility assays

To assess kinesin function, standard microtubule gliding assays were employed as previously described (2). Briefly, flow cells were constructed from microscope slides (Fisher), glass coverslips (Corning 1 1/2, 18 mm^2) and double-sided tape. First, 0.5 mg/mL casein was introduced and incubated for 3–5 min, followed by kinesin motors diluted in 0.2 mg/mL casein and 0.1 mM ATP, followed by motility solution (32 nM fluorescent microtubules, 1 mM ATP, 0.2 mg/mL casein, 10 μM taxol, and antifade cocktail consisting of 20 mM D-glucose, 0.02 mg/mL glucose oxidase, 0.008 mg/mL catalase, and 0.5% β-mercaptoethanol). Microtubules were visualized using a Nikon E600 upright microscope with a 100$\times$ 1.3 NA oil objective. Images were captured to videotape using a Genwac GW-902H camera and analyzed offline.

QCM sensor surface

For the QCM experiments, AT-cut (thickness-shear mode) quartz crystals with a fundamental frequency of 27 MHz were coated with SiO_2. These crystals have an 8.7-mm-diameter crystal plate and are covered by a

0.049 cm^2 Au electrode. To improve the adhesion between the gold surfaces and SiO_2 films, the sensor surfaces were cleaned with UV irradiation for 15 min. After cleaning, a 100-nm SiO_2 layer was deposited onto the Au surface using plasma chemical vapor deposition (ULVAC, CC-200). The thickness of the SiO_2 layer was verified by monitoring the fundamental frequency of crystals using the QCM system. Before each use, the sensor surfaces were cleaned with a 1% SDS solution followed by piranha solution (H_2SO_4/30% H_2O_2 = 3:1) to remove organic contamination, followed by several rinses with distilled water.

QCM Instrument

QCM measurements were performed with an AFFINIX Q4 instrument (Initium, Tokyo, Japan). This instrument has four 500-μL cells equipped with a 27 MHz QCM plate at the bottom of each cell along with a stirring bar and temperature control system. Sauerbrey's equation was obtained for the AT-cut shear-mode QCM in the air phase,

$$\Delta F = -\frac{2F_0^2\Delta m}{A\sqrt{\rho_q\mu_q}}, \quad (1)$$

where ΔF is the measured frequency change (Hz), F_0 is the fundamental frequency of the quartz crystal (27 MHz), Δm is the mass change, A is the electrode area (0.049 cm^2), ρ_q is the density of quartz (2.65 g cm^{-3}), and μ_q is the shear modulus of quartz (2.95×10^{11} dyne cm^{-2}) (40). From Eq. 1, a 0.62 ng cm^{-2} increase in mass results in a 1-Hz decrease in frequency in air. The peak-to-peak noise of the 27-MHz QCM was 3 Hz in buffer at 25°C.

Casein, kinesin, and microtubule binding

Before protein binding measurements, the SiO_2-coated QCM sensor was equilibrated by incubating BRB80 buffer in the chamber at 25°C for 20 min. Next, casein was introduced into each chamber, and the resulting frequency decrease was recorded over the next 10–60 min. After casein adsorption, any unbound casein was washed out by replacing the buffer solution in the chamber five times. Reversible casein and motor binding was assessed by adding different solutions to QCM chambers previously treated with casein. Kinesin motor proteins (full-length, headless and tailless) were prepared in BRB80 buffer with or without 0.2 mg/mL casein, and were introduced into the QCM sensor cells. After binding, unbound proteins were removed by replacing the solution five times with motor-free buffer.

Quantifying casein binding affinity

The interaction of casein in solution ($Cs_{Solution}$) with the tightly bound monolayer of casein on the surface (Cs_{Tight}) to form a bilayer of tightly and weakly bound casein (Cs_{Weak}-Cs_{Tight}) was expressed as a reversible binding interaction:

$$Cs_{Solution} + Cs_{Tight} \underset{k_{off}}{\overset{k_{on}}{\rightleftarrows}} Cs_{Weak}\text{-}Cs_{Tight}.$$

Equilibrium casein binding data were fit to a Langmuir isotherm:

$$\Delta F = \frac{K_A[Cs_{Solution}]}{1 + K_A[Cs_{Solution}]} \times \Delta F_{max}, \quad (2)$$

where ΔF is the measured frequency change, $[Cs_{Solution}]$ is the concentration of casein in solution, and K_A is the association constant (in M^{-1}). The kinetics of reversible casein binding was assessed by introducing different concentrations of casein in solution and measuring the time course of the frequency change. The kinetics was analyzed as follows:

$$[Cs_{Weak}\text{-}Cs_{Tight}] = [Cs_{Weak}\text{-}Cs_{Tight}]_{max}\left(1 - e^{(-t/\tau)}\right) \quad (3)$$

$$\Delta F = \Delta F_{max}\left(1 - e^{(-t/\tau)}\right) \quad (4)$$

$$1/\tau = k_{on}[Cs_{Solution}] + k_{off}. \quad (5)$$

Time constants for casein binding (τ) were obtained by fitting the time course of casein binding (see Fig. 3 *b*, *inset*) with Eq. 4. Rate constants for the reversible binding of weakly bound casein (k_{off} and k_{on} in Table 1) were obtained by fitting Eq. 5 to these data (see Fig. 3 *c*).

Dynamic light scattering

Dynamic light scattering (DLS) measurements were used to characterize the size of casein aggregates in solution. DLS measurements were performed using a Zetasizer Nano (Malvern Instruments, Worcestershire, UK) with 1 mL of 0.2 mg/mL casein solution in BRB80 buffer at 25°C. An intensity autocorrelation curve was generated and transformed to a volume distribution of casein aggregates in solution.

RESULTS

Casein maximizes the activity of surface-bound kinesin

As a first test of casein function, we compared the ability of casein and BSA to maintain the activity of surface-adsorbed kinesin in the microtubule gliding assay. In what we define here as the ''standard'' microtubule gliding assay, which is used routinely in a number of labs and is the protocol presented on the Kinesin Home Page (http://www.proweb.org/kinesin//), surfaces are pretreated with 0.5 mg/mL casein, and 0.2 mg/mL casein is also included in the motor solution and the microtubule solution (2,17). Using this protocol, robust microtubule gliding is observed using kinesin concentrations well below 1 μg/mL (2). It is known that adsorbing kinesin in the absence of any blocking agent results in very low motor activity, presumably due to motor denaturation on the surface (3). BSA has been used as a blocking agent by Böhm et al., and although robust microtubule gliding was observed when high kinesin concentrations were employed, no microtubule motility was observed when kinesin concentrations below 10 μg/mL were used (41).

To quantify the degree to which casein maximizes the activity of surface-adsorbed kinesin, we replaced the casein in the blocking solution, motor solution, and microtubule solution with 0.5 mg/mL BSA. Because this concentration

TABLE 1 Rate constants and binding affinity of tightly and weakly bound casein on the QCM surface

	k_{on} (10^3 $M^{-1}s^{-1}$)	k_{off} (10^{-3} s^{-1})	K_A (10^6 M^{-1})	K_D (nM)	Δm (ng cm^{-2})
Tightly bound casein	n.d.	n.d.	140*	7.1*	279*
Weakly bound casein	5.4†	3.5†	2.0‡	500‡	102‡

Data represent fits to data in Fig. 3, as described in Methods. $K_D = 1/K_A$.
*Values determined from Fig. 3 *a*.
†Values determined from Fig. 3 *c*.
‡Values determined from Fig. 3 *b*.

is ~5-fold higher than the amount of BSA needed to form a continuous 4-nm-thick surface monolayer, this treatment is expected to completely block the surface. To quantify kinesin activity, we measured the number of microtubules moving over a surface coated with 5 μg/mL full-length kinesin after 5 min of incubation. The microtubule landing rate has been shown to vary with kinesin concentration up to a plateau where microtubule landing is diffusion limited (2,3), meaning that the microtubule landing rate can be used as a measure of the concentration of active motors on the surface. As seen in Fig. 1, using identical 5 μg/mL kinesin concentrations, BSA treatment resulted in drastically fewer microtubules bound to the surface. To quantify the enhancement of motor activity more precisely, we decreased the kinesin concentration in casein to match the results seen with BSA and found that the activity of 0.1 μg/mL kinesin in casein matched the activity of 5 μg/mL kinesin in BSA. This result indicates that the functional activity achieved per motor introduced into the flow cell is 50-fold higher when the motility assay is performed with casein rather than BSA.

Casein binding to surfaces as measured by QCM

In the gliding assays shown in Fig. 1, casein is used to pretreat the surface and is included in both the kinesin solution and the microtubule solution. If casein binds reversibly to the surface, then it may be important to maintain sufficient casein concentrations in the assay to prevent the motor domains from binding to the surface and inactivating. However, the reversibility of casein surface adsorption has not been well characterized. To precisely quantify the amount and the affinity of casein binding to glass surfaces, we measured the binding of casein to a SiO_2 functionalized quartz electrode in a quartz crystal microbalance (QCM) instrument. The simple prediction is that, above a minimum casein concentration, an irreversible monolayer will form with a thickness corresponding to the size of casein in solution. To measure this surface binding, varying concentrations of casein were introduced into the QCM measurement cell and the resulting change in resonant frequency measured before and after washout with buffer. The first goal was to measure the amount of casein bound when the electrode was incubated in saturating concentrations of casein (analogous to the conditions of the gliding assay), and the second goal was to assess the extent to which casein binding to the surface is reversible.

Fig. 2 shows a typical trace from the QCM experiments. When a 0.2 mg/mL casein solution is introduced into the sample chamber, there is a rapid fall in the resonant frequency by ~1500 Hz, corresponding to an increase in mass from protein binding to the SiO_2 surface. After ~35 min, the casein solution is replaced with protein-free buffer and rinsed five times to remove any weakly bound protein. At this point, the frequency rises by ~300 Hz, indicating that most of the protein is tightly bound to the surface. Finally, after introduction of a new 0.2 mg/mL casein solution at 60 min, the frequency again falls, indicating the reversible binding of a weakly bound casein layer. These data suggest that there are two modes of casein binding to SiO_2 surfaces, a tightly bound layer (with magnitude $a - c$ in Fig. 2) and a weakly bound layer (with magnitude $c - b$ in Fig. 2).

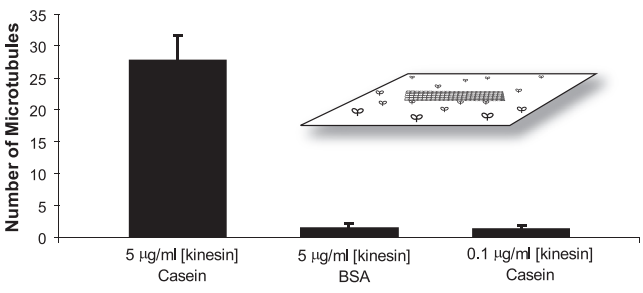

FIGURE 1 Comparing the microtubule-binding activity of kinesin in casein and BSA. In the casein experiment, flow cells were pretreated with 0.5 mg/mL casein, and 0.2 mg/mL casein was present in both the kinesin and microtubule solutions. In the BSA experiment, casein was replaced by 0.5 mg/mL BSA in all solutions. Five minutes after introduction of rhodamine-labeled microtubules (64 nM), the number of microtubules moving in each 70 μm × 55 μm video screen was counted. Data for each condition are plotted as mean ± SD for $N = 30$ windows taken from three different flow cells. (*Inset*) Diagram of the microtubule gliding assay.

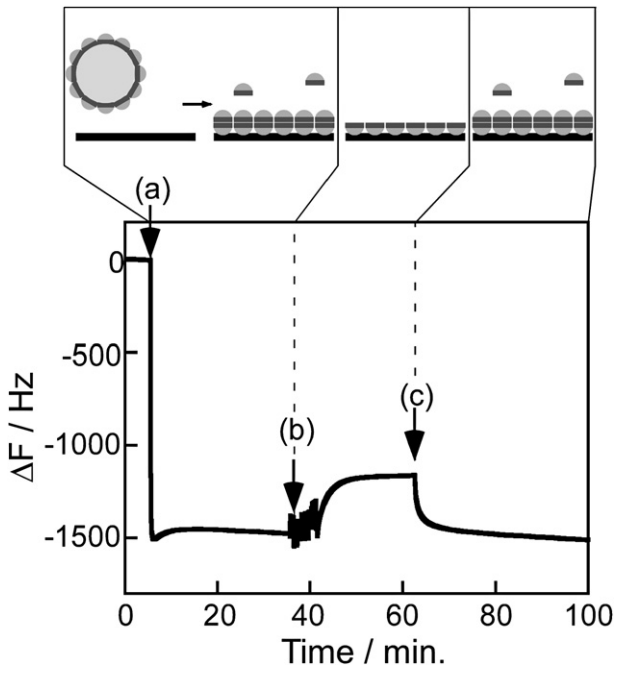

FIGURE 2 Typical real-time monitoring of casein binding to a SiO_2 surface in the QCM. (*a*) Addition of 0.2 mg/mL casein solution, (*b*) wash with casein-free buffer, (*c*) wash in of 0.2 mg/mL casein solution. Panels illustrate model for casein submicelles in solution landing and dissociating on the surface to form a tightly bound monolayer and a weakly bound secondary layer. In a separate experiment using a surface-passivated QCM electrode, introducing a 0.2 mg/mL BSA solution resulted in no frequency change (data not shown), indicating that the observed response is caused by surface binding of casein and not by changes in solution viscosity or density.

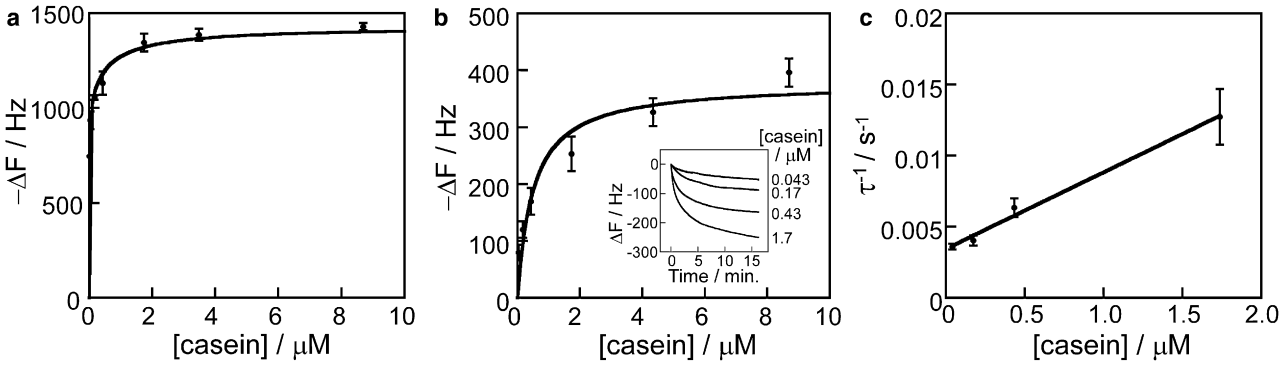

FIGURE 3 Casein surface binding isotherms. (*a*) Frequency change resulting from casein binding to the SiO_2 surface of the QCM. Frequency data, corresponding to the time just before point *b* in Fig. 2, are presented as a function of the initial casein concentration in solution. (*b*) Binding of the reversible casein layer onto a casein-coated SiO_2 surface. *Inset* shows raw traces, demonstrating the kinetics of casein binding. Data are presented as mean ± SD for three to five determinations each. (*c*) Linear reciprocal plots of the time constant (taken from *b, inset*) versus casein concentration. Fit parameters are given in Table 1.

To more fully investigate the kinetics and affinity of casein binding to the SiO_2 surface, different concentrations of casein were incubated in the experimental chamber, and the resulting frequency changes were recorded. From Fig. 3 *a*, casein binding saturates at ~1500 Hz. Fig. 3 *b* shows a binding isotherm for reversibly bound casein, determined by preincubating the surface with a saturating concentration of protein, washing with casein-free buffer, and then introducing solutions with varying casein concentrations. A fit to the data gave a maximum frequency change of 378 Hz and a dissociation constant of 500 nM, assuming a 24 kDa average subunit molecular mass. The magnitude and affinity of the tightly bound casein layer were calculated by subtracting the reversibly bound casein in Fig. 3 *b* from the total bound casein in Fig. 3 *a*. The tightly bound casein layer had an affinity of 7 nM and had a maximal frequency change of 1078 Hz; however, because of the potential for solution depletion at very low concentrations, we consider this 7 nM to be an upper limit, and the affinity may be considerably tighter than this.

The calculated equilibrium binding constants and rate constants for casein binding to the SiO_2 surface in the QCM are presented in Table 1. For dissociation of the reversibly bound layer, the k_{off} of 3.5×10^{-3} s^{-1} corresponds to a time constant of ~5 min. We were unable to measure the kinetics of the tightly bound layer, but as >60 min washes in protein-free buffer led to negligible dissociation of this tightly bound casein (data not shown), this tightly bound layer was, for all practical purposes, irreversibly bound. Notably, the 500 nM dissociation constant for weakly bound casein corresponds to 0.011 mg/mL casein, which is more than 10-fold below the 0.2 mg/mL routinely used in motility assays. This means that under standard conditions used in motility assays, both a tightly bound layer and a weakly bound layer of casein are adsorbed to the surface.

If we consider casein binding to be monolayer surface coverage, what are the thicknesses of the tightly and weakly bound casein layers? In air, changes in the QCM resonant frequency correspond well to changes in the mass of the crystal and can be quantified by the Sauerbrey Equation (see Methods). However, in aqueous solutions, changes in the resonant frequency not only correspond to mass changes resulting from bound proteins but also involve the hydration layer and the viscoelasticity of the adsorbed protein (42). To account for these hydrodynamic effects, we directly calibrated the relation between ΔF in water and ΔF in air after adsorption of varying amounts of casein on the surface of the 27-MHz QCM crystal and found that the frequency changes in solution are 2.3 times the frequency change in the air. This result agrees well with measurements from a range of proteins that had factors ranging from 1.8 to 4.7 and nearly matches the factor of 2.5 observed for BSA (42). Using Eq. 1 and this factor of 2.3 for $\Delta F_{water}/\Delta F_{air}$ gives a conversion factor of 0.27 ng/cm^2/Hz for the 0.049 cm^2 electrode, so the 1035 Hz from the tightly bound casein layer corresponds to 279 ng/cm^2 on the crystal surface. Assuming that the density of the hydrated protein layer on the surface is 1.35 g/cm^3 (43), this mass change corresponds to a 2.1 nm thick tightly bound casein layer on the QCM surface. The 378 Hz maximal signal for reversibly bound casein, corresponding to 102 ng/cm^2, is one-third of this and can be interpreted either as a second layer with one-third the thickness or a one-third coverage at the same thickness as the first layer.

Characterizing casein in solution

Under different conditions, casein can take on a range of structural states from nanometer-scale monomers to micelles hundreds of nanometers in size. To better understand the structure of soluble and surface-bound casein in our experiments, we investigated the subunit composition and the solution aggregation state of our casein protein. Our standard protocol involves dissolving casein overnight in calcium-free buffer, centrifuging to remove large aggregates, and finally filtering through 0.22-μm syringe filters. This

TABLE 2 Molecular mass and composition of casein subunits in bovine milk

Subunit	Molecular mass (kDa)	Composition in milk (g/L)
α_{s1}	22–23.6	12–15
α_{s2}	25	3–4
β	24	9–11
κ	19	2–4

Data from Eigler et al. (52).

protocol is expected to remove the micelles and large complexes found in milk, but the resulting protein could be present as 3–4-nm casein monomers, ''submicelle particles'' in the 5–50-nm size range, or potentially larger aggregates (20,21,24).

One determinant of the aggregation state is the casein subunit composition. Whole casein includes α-, β-, and κ-casein subunits, and there are a number of models that describe the roles that each plays. Table 2 gives sizes of the various casein subunits and their approximate stoichiometries in milk. To determine the subunit composition of our filtered whole casein, we ran an SDS-PAGE gel of our filtered casein along with isolated α-, β-, and κ-casein. As seen in Fig. 4 *b*, α-casein runs at 25 kDa (presumably this is α_{S2} at 25 kDa), β-casein runs at ~23 kDa along with a faint band at ~32 kDa, and κ-casein runs at 21 kDa. The filtered whole casein used in this work (lane 2) consists primarily of α- and β-casein with little κ-casein present.

To assess the aggregation state of filtered casein in solution, we carried out dynamic light-scattering measurements of casein at the 0.2 mg/mL concentration used in our experiments. As seen in Fig. 4 *a*, the majority of the protein is found in aggregates centered around 16 nm, with the wide peak ranging from <10 nm up to nearly 40 nm. There is a small peak in the data centered at 182 nm (0.3% of the total protein volume) and 4690 nm (0.1% of the total protein volume). Importantly, there is no evidence of aggregates smaller than 8 nm, meaning that 20–30-kDa soluble casein monomers, which are expected to be in the 3–4-nm range, appear not to be present in solution. From electron microscopy studies, the term ''submicelle'' has been used to describe aggregates of casein monomers that come together to form casein micelles, although the size and subunit constitution of these submicelles are not well defined (20,21, 24–26,44). We interpret the 16-nm casein aggregates identified by dynamic light scattering to be submicelle particles, each containing tens of casein monomers.

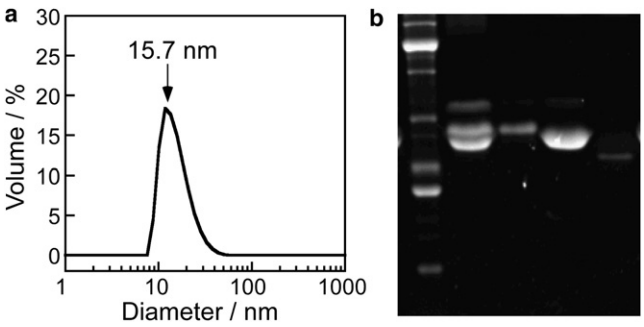

FIGURE 4 Characterizing casein in solution. (*a*) Dynamic light scattering of 0.2 mg/mL casein in BRB80 buffer at 25°C. The peak centered at 15.7 nm accounts for >99.5% of the particle volume; there are also small peaks centered at 182 nm and 4690 nm, accounting for 0.3% and 0.1%, respectively. No detectable signal was seen below 8 nm. (*b*) SDS-PAGE gel of casein in solution. Lane 1 is molecular mass marker, lane 2 is filtered whole casein used in this study, lane 3 is α casein, lane 4 is β-casein, and lane 5 is κ-casein.

How can the 16-nm aggregates measured in solution be reconciled with the 279 ng/cm^2 surface-bound casein measured from the QCM measurements? A rectangular array of 16-nm-diameter spherical protein particles would correspond to a surface coverage of 1130 ng/cm^2, and even a 55% surface coverage as predicted from random parking models (45) corresponds to 792 ng/cm^2. The results can be understood if the submicelles, on interacting with the surface, dissociate into their respective subunits, and it is these casein monomers that create a surface monolayer. The average molecular mass of the casein subunits is 24 kDa, which corresponds to a spherical protein with a diameter of 3.8 nm or a cuboidal protein, 3.1 nm on a side. Perfect packing of these cubes (a 3.1-nm monolayer) corresponds to a mass of 418 ng/cm^2, and looser packing such as a rectangular lattice of spheres corresponds to 268 ng/cm^2. Hence, the measured 279 ng/cm^2 mass of tightly bound casein is quantitatively consistent with casein submicelles dissociating into subunits on binding to the surface.

Measuring kinesin surface binding by QCM

To understand the interaction of kinesin motors with surface-adsorbed casein, we used QCM to measure the binding of full-length and truncated kinesin to casein-treated surfaces. In the conventional model, casein pretreatment enables kinesin tails to bind to the surface while preventing the heads from binding to the surface. The evidence for this model is the fact that surface-adsorbed kinesin is functional and is able to move microtubules across the surface. However, the data do not preclude the possibility that motors bind nonspecifically, such that half of the motors are pointed up and half are pointed down. In any case, the mechanism by which casein alters the binding of kinesin heads or tails to glass surfaces is not understood. We addressed this question by pretreating surfaces with a saturating concentration of casein to form a tightly bound layer of casein on the surface and then washing in motors in either the presence or absence of casein. To assess the contribution of kinesin head binding versus kinesin tail binding, we repeated the experiments with a headless construct (missing the first 340 residues (2)) and a tailless construct (truncated at residue 559 (37)).

Motor binding traces are shown in Fig. 5. In all cases, clean SiO_2 surfaces were treated with casein to form a tightly bound casein layer on the surface before adding motors. For full-length kinesin, a similar degree of motor binding was

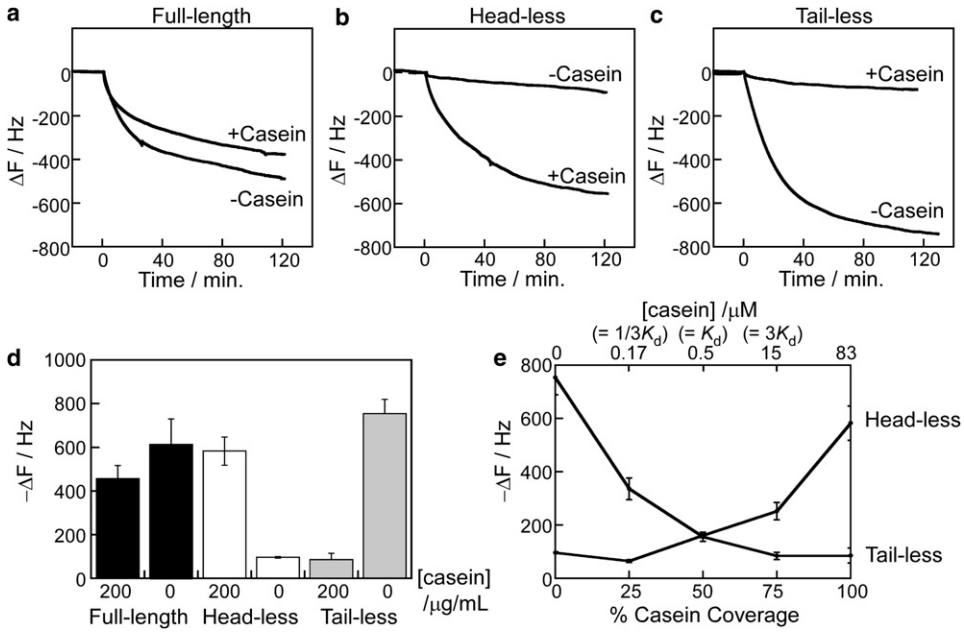

FIGURE 5 Binding of kinesin to casein-treated SiO_2 QCM surface in the presence and absence of casein in solution. (*a*) Full-length kinesin, (*b*) headless kinesin, (*c*) tailless kinesin in 0 or 0.2 mg/mL casein. (*d*) Summary of kinesin binding after 2 h in 0 or 0.2 mg/mL casein shown as mean ± SD from three determinations for each condition. (*e*) Binding of headless and tailless kinesin to casein-treated SiO_2 surface in the presence of varying casein concentrations in solution. Data are plotted as percentage surface coverage using the K_D of 0.5 μM in Table 1. For all experiments, [kinesin] = 3.7 nM, [casein] = 0 or 0.2 mg/mL, and [AMP-PNP] = 0.1 mM in BRB80 buffer at 25°C.

observed in the presence and absence of soluble casein after 2 h of incubation. Interestingly, in the presence of casein, which matches normal conditions in the microtubule gliding assay, the measured 450 Hz (corresponding to 121 ng/cm^2 of protein using the 0.27 ng/cm^2/Hz QCM response in water) corresponds to a coverage of ~3000 kinesin dimers (223 kDa) per square micrometer. This agrees well with a previous estimate from functional assays that measured the saturating coverage of full-length kinesin motors to be 2000 motors/μm^2 (2). To better understand how full-length kinesin binds to the casein-pretreated SiO_2 surface, the binding of headless and tailless kinesin was measured in the presence and absence of soluble casein. In the presence of casein, headless kinesin bound to the surface to a similar degree as full-length kinesin, but interestingly, in the absence of casein, very little headless kinesin bound to the surface (Fig. 5 *b*). This result is somewhat counterintuitive: despite the presence of a tightly bound layer of casein on the surface, very little kinesin tail binds if soluble casein (and presumably the weakly bound casein layer) is not present.

In contrast to headless kinesin, tailless kinesin binds well to the surface when soluble casein is absent, but in the presence of soluble casein, the kinesin heads do not bind to the surface (Fig. 5 *c*). This result is broadly consistent with the idea that surface-bound casein prevents kinesin head binding (and head inactivation); however, the difference is that the surface contains a layer of tightly bound casein, and it is the casein in solution (or the weakly bound casein layer) that blocks the kinesin head from binding to the surface. The results for binding of all three motor constructs in the presence and absence of soluble casein are shown in Fig. 5 *d*.

To uncover the mechanism by which weakly bound casein controls kinesin surface binding, headless and tailless kinesin were incubated in the presence of varying concentrations of free casein (Fig. 5 *e*). If soluble casein and kinesin heads compete for the same area on the casein-treated surface, then a simple prediction would be that 50% surface coverage of the casein secondary layer would result in half-maximal kinesin head binding. Similarly, if weakly bound casein promotes kinesin tail binding to the casein-treated surface, then 50% coverage of a weakly bound casein layer would be predicted to result in half of the kinesin tail binding to the surface. The data are inconsistent with both of these predictions. At 0.5 μM casein, which corresponds to the formation of 50% of the weakly bound layer (see Fig. 3), adsorption of the kinesin head to the surface was almost fully prevented, ruling out a model by which weakly bound casein competes with kinesin heads for available surface binding sites and suggesting a cooperative mechanism by which relatively small amounts of weakly bound casein significantly block kinesin head binding to the surface. Likewise, at casein concentrations corresponding to a 50% weakly bound layer, very little kinesin tail binds to the surface, suggesting that a nearly saturating weakly bound layer of casein is needed to enable kinesin tail surface binding.

Measuring the reversibility of headless and tailless kinesin binding

To better understand the interaction of kinesin head and tail domains with casein-treated surfaces, we measured the reversibility of headless and tailless kinesin binding using the QCM. The finding that in the absence of a weakly bound layer of casein, very little headless kinesin binds to the surface (Fig. 5 *b*) suggests that the kinesin tail actually binds to the surface via the reversibly bound casein layer. If this were the case, then washing out the reversibly bound casein should remove a substantial fraction of the headless kinesin

from the surface. This prediction was tested in Fig. 6 *a*. At point 1, headless kinesin (3.7 nM) was washed into a casein-pretreated surface in the presence of 0.2 mg/mL casein. Consistent with Fig. 5 *b*, the frequency falls by ~600 Hz, indicating headless kinesin binding. After a wash to remove any unbound motor, the buffer was replaced by casein-free buffer. If the headless kinesin were bound to the reversibly bound casein, then this step should wash both the casein and the headless motors off of the surface. Instead, at point 3 the frequency only rises by ~250 Hz, slightly less than the degree of reversible casein binding seen in Fig. 3 *b*. If both the reversibly bound casein and the headless kinesin dissociated from the surface at point 3, the resulting frequency change would be a sum of the casein dissociation (~250 Hz) and the headless kinesin dissociation (~650 Hz from point 1 to point 2). Hence, headless kinesin does not dissociate from the surface in casein-free buffer, strongly suggesting that the kinesin tail does not bind solely to the reversibly bound casein layer on the surface.

We next tested whether the kinesin head binding observed in Fig. 5 *c* is reversible. In that experiment, tailless kinesin bound to a casein-treated surface only in the absence of soluble casein. One possibility is that this binding is weak and reversed simply by washing out the motors; alternatively, soluble casein could reverse this head binding by forming a reversibly bound casein layer on the surface that resists kinesin head binding. In Fig. 6 *b*, the surface was first pretreated with a saturating casein solution, followed by a casein-free wash to establish a tightly bound casein monolayer. At point 4, tailless kinesin was introduced, and the frequency fell by ~700 Hz, consistent with the tailless kinesin binding seen in Fig. 5 *c*. Washing out the motor solution with casein-free buffer (point 5) resulted in a frequency rise of ~150 Hz, indicating that ~20% of the kinesin heads are reversibly bound. Next, in an attempt to displace the remaining kinesin heads from the surface, a 0.2 mg/mL casein solution was introduced at point 6. The resulting 350-Hz fall (consistent with the reversible casein binding in Fig. 3 *b*) is interpreted to mean that 1), casein binds reversibly to the surface to the same degree in the presence and absence of surface-bound motor heads, and 2), introducing casein does not immediately displace the kinesin heads from the surface. To further confirm that the soluble casein does not displace the motors, the flow cell was washed at point 7 with casein-free buffer. The resulting small frequency increase is consistent with only the reversibly bound casein being washed off of the surface. Hence, whereas ~20% of the kinesin heads are reversibly bound in the absence of soluble casein, the remaining 80% of the heads are not reversibly bound to the surface.

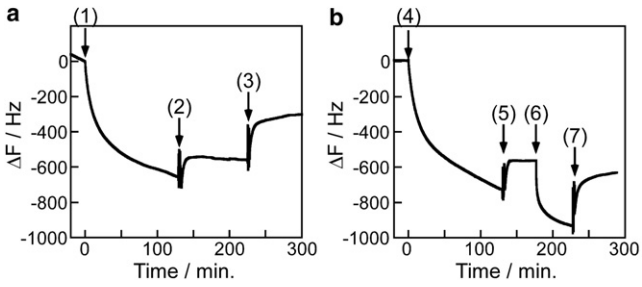

FIGURE 6 Testing the reversibility of kinesin head and tail binding. (*a*) To test kinesin tail binding, 3.7 nM headless kinesin was washed onto a casein-pretreated SiO_2 surface in the presence of 0.2 mg/mL casein (point 1). Note that because the solution preceding point 1 contained 0.2 mg/mL casein, the frequency change is caused solely by headless kinesin binding. At point 2, the solution was replaced with kinesin-free buffer containing 0.2 mg/mL casein to remove any unbound headless kinesin. At point 3, the solution was replaced with casein-free buffer to test whether casein dissociation resulted in kinesin dissociation. (*b*) To test kinesin head binding, 3.7 nM tailless kinesin was washed onto a casein-pretreated surface in casein-free buffer (point 4). At point 5, motor-free buffer was washed in, and at point 6, 0.2 mg/mL casein solution was washed in in an attempt to displace the bound motors. At point 7, solution was replaced by casein-free buffer to remove any motors that had been displaced by the soluble casein.

Assessing functional activity of adsorbed kinesin by QCM

We next addressed the question: what is the relative activity of kinesin adsorbed to surfaces in the presence and absence of casein? From Fig. 5 *a*, comparable amounts of full-length kinesin bind to the QCM sensor surface in the presence and absence of soluble casein, and the simple interpretation is that in the presence of casein the motors bind through their tail domain, whereas in the absence of casein the motors bind through their head domains. The prediction is that motors adsorbed in the presence of casein will be functional (tail down, head up), whereas motors adsorbed in the absence of casein will be nonfunctional (tail up, head down). To test this prediction, we used the QCM to assess the ability of immobilized full-length kinesin to bind microtubules in the presence of the nonhydrolyzable ATP analog AMP-PNP. Under these conditions, functional motors should bind microtubules irreversibly to the surface, resulting in a detectable mass increase. The limit of detection in this instrument is ~3 Hz, which corresponds to 39 pg of protein binding to the QCM crystal. This mass corresponds to ~26,000 microtubules with mean lengths of 5 μm or, equivalently, to a 0.07% surface coverage of the 0.049 cm^2 crystal. As seen in Fig. 7, after 1 h of incubation, the motors adsorbed in the presence of casein bound 5–10 times more microtubules than the motors adsorbed in the absence of casein, consistent with predictions.

Weakly bound casein enhances the activity of surface-adsorbed kinesin

The QCM data in Fig. 7 indicate that the functional activity of adsorbed kinesin motors is severely diminished when casein is absent in the kinesin and microtubule solutions, implying that simply pretreating a surface with casein is

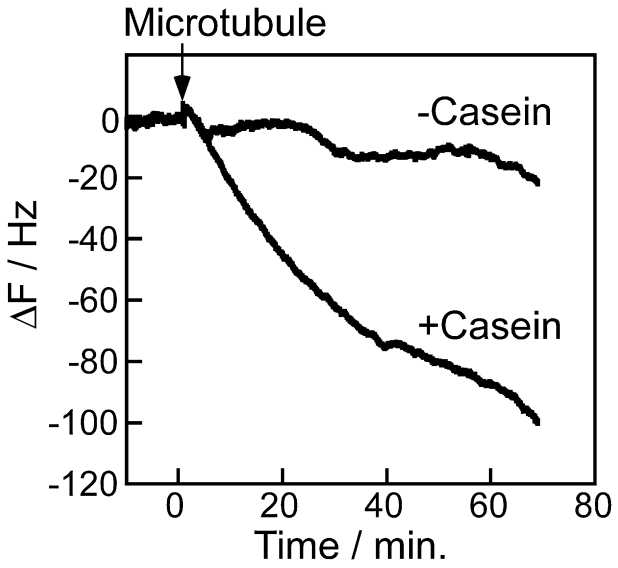

FIGURE 7 Binding of microtubules to kinesin immobilized on the SiO_2 QCM surface. Both surfaces were pretreated with a saturating casein concentration, washed with casein-free buffer, and then kinesin and microtubules were introduced. In the +Casein experiment, 0.2 mg/mL casein was present in both the kinesin and microtubule solutions. In the −Casein experiment, casein was left out of both the kinesin and microtubule solutions. In both experiments, 0.1 μM taxol-stabilized microtubules and 3.7 nM full-length kinesin motors were used, and all solutions contained 0.1 mM AMP-PNP to maximize microtubule binding.

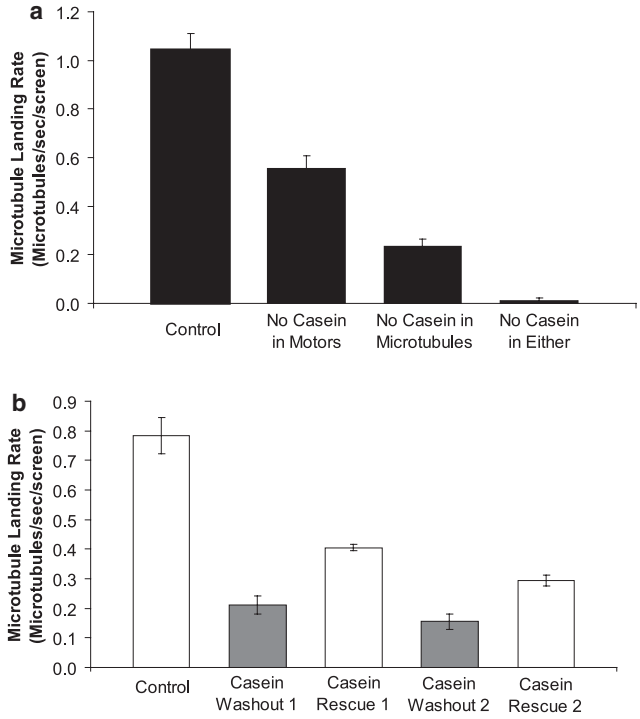

FIGURE 8 (*a*) Importance of soluble casein in the kinesin and microtubule solutions. For the control experiment, a standard motility assay was run using 0.5 mg/mL casein pretreatment, 0.2 mg/mL casein in the kinesin solution (5 μg/mL full-length kinesin), and 0.2 mg/mL casein in the microtubule solution. Casein was then left out of either the kinesin solution, the microtubule solution, or both. In each case, the rate that microtubules landed and moved was measured and plotted as mean for $N = 6$ screens (70 μm × 55 μm) from two flow cells. In all cases, every microtubule that landed moved over the surface. (*b*) The reversibility of casein enhancement. In a standard gliding assay, the casein-containing microtubule solution was washed out and replaced with a casein-free motility solution, and the microtubule landing rate was determined. New microtubule solution containing 0.2 mg/mL casein was then washed in to rescue the motility, and the process was repeated. Data are mean ± SD for three screens each. Because of sparse surface coverage of microtubules and replenishment in new solutions, the instantaneous microtubule landing rates are expected to be independent of the number of microtubules that have previously landed.

not sufficient to maximize kinesin functionality. However, it leaves open the question of whether the presence of a reversibly bound casein layer is important during the kinesin adsorption step or during the time when surface-adsorbed kinesin is interacting with microtubules (or both). To address this question, we turned to microtubule gliding assays to more precisely quantify kinesin activity. Because conventional kinesin is a processive motor, below a certain motor surface density the rate that microtubules land on and move over the surface is proportional to the kinesin motor density on the surface (2,3). Hence, the microtubule landing rate can be used as a measure of the concentration of active motors on the surface.

The data in Fig. 8 complement and extend the QCM results from Fig. 7. In all cases, surfaces were pretreated with 0.5 mg/mL casein. When casein was left out of both the kinesin solution and the microtubule solution, the landing rate was 100-fold lower than the control case. This agrees well with the lack of microtubule binding seen in Fig. 7 and reinforces that simply pretreating the surface with casein is not sufficient to maximize the function of surface-adsorbed kinesin. To test whether the reversibly bound casein layer exerts its effect during the kinesin adsorption step or during the microtubule binding step, soluble casein was left out of either the kinesin solution or the microtubule solution. When casein was left out of the kinesin solution, the landing rate was 53% of control, but when casein was left out of the microtubule solution, the landing rate fell to 22% of control. Hence, the dominant effect of the reversibly bound casein layer in maximizing kinesin activity was not enhancement of kinesin adsorption but was instead an enhancement of the activity of surface-adsorbed motors. These results are consistent with similar experiments by Verma et al. (23).

To better understand how the presence of soluble casein enhances the activity of surface-adsorbed kinesin, we asked the question: is this enhancement reversible? If, in the absence of weakly bound casein the motor heads become irreversibly stuck, then adding back soluble casein should have no effect. On the other hand, if the motor heads inactivate by reversibly binding to the surface, or if soluble casein stabilizes the secondary structure of kinesin, then adding back soluble casein should rescue the motor activity. To test this reversibility, the standard gliding assay was run, the casein-containing microtubule solution was then

replaced by casein-free microtubule solution, and finally, this solution was replaced by normal casein-containing microtubule solution. As seen in Fig. 8 *b*, the casein-free microtubule solution resulted in a decrease of motor activity to 27% of control, as expected, and washing back in the casein-containing solution brought the activity up to 52% of control. Hence, the reduction in kinesin activity is reversible to a degree, and a second cycle of casein-free and casein-containing microtubule solution shows a similar rescue to ~50% of the initial level. The fact that the rescue of activity is not fully reversible suggests that some motor heads may irreversibly bind to the surface in the absence of soluble casein. However, the reversibility implies that either most motor heads bind reversibly to the casein monolayer or that soluble casein may stabilize the secondary structure of immobilized kinesin.

DISCUSSION

With the development of novel in vitro assays of protein function and the push toward shrinking clinical tests down to lab-on-a-chip dimensions, there is a growing need to understand the mechanisms by which artificial surfaces modulate the activity of adsorbed proteins. Understanding the role that casein plays in maximizing the function of surface-adsorbed kinesin is important because this assay is a model for studying motor proteins in vitro. The robust activity of surface-adsorbed kinesins and the avidity with which they bind to silica and polystyrene surfaces has enabled mechanical studies that exert piconewton-level forces on these motors (46,47). Because the kinesin tail domain is positively charged (the C-terminal 65 residues of *Drosophila* conventional kinesin has a net charge of +9), it has often been assumed that charge interactions mediate kinesin tail binding to SiO_2 surfaces. By quantifying both the functional activity of immobilized kinesin motors and the adsorption profiles of motors and casein to surfaces, we find that the picture is much more complex. QCM experiments demonstrate that casein adsorbs to SiO_2 surfaces as a tightly bound layer consistent with a monolayer of isolated casein subunits, and in the presence of soluble casein, a second, reversibly bound layer also adsorbs. This weakly bound casein layer enhances binding of the kinesin tail domain to the surface and inhibits the binding of the kinesin head domains to the surface. Furthermore, the microtubule-binding activity of surface-adsorbed kinesin can be reversibly modulated by removing and replacing the reversibly bound casein layer. The results presented here are interpreted in the context of the model shown in Fig. 9.

Casein binds to SiO_2 surfaces as a tightly bound and a reversibly bound layer

Although casein can take on many forms in solution, the light scattering and electrophoresis data in Fig. 4 indicate that the filtered casein in BRB80 buffer generally used in kinesin experiments exists as aggregates of predominantly α- and β-casein with a mean diameter of 16 nm. Three decades of casein research has generated numerous models and continuing debates regarding the structure of casein in solution. No crystal structures are available for any of the casein subunits, and to varying degrees the isolated subunits are all thought to take on somewhat unstructured conformations in solution (21,24,33,48). In milk, casein forms micelles that sequester calcium. One class of models describes the micelle structure as a shell of α- and β-casein on the surface with κ-casein in the middle. A second class of models describes the micelle as an aggregate of smaller (submicelle) particles akin to a raspberry (20,21,25). For simplicity, we refer to our 16-nm aggregates as submicelle particles, but our experiments provide little fuel to ongoing debates regarding the structure of native casein micelles in milk. We do note that casein subunits, particularly β-casein, are known to be amphipathic and have surfactant properties (33). In our working model, it is these surfactant properties that both stabilize the 16-nm casein micelles in solution and govern the interactions between casein subunits and the surface.

From the casein binding data in Fig. 3 and Table 2, a model for the interaction of casein with glass and SiO_2 surfaces emerges. On a clean surface, casein binds up to a maximum surface coverage of 380 ng/cm^2, and, after extensive washing with casein-free buffer, a surface monolayer of 279 ng/cm^2 remains. This mass of this remaining casein is consistent with rectangular packing of 3.8-nm spheres creating a tightly bound monolayer of casein subunits on the surface. The reversibly bound layer of casein has a mass of one-third of the tightly bound casein layer and binds with a dissociation constant of 500 nM. These results are in reasonable agreement with results from Tiberg et al., who used neutron scattering to measure adsorption of pure β-casein to SiO_2 surfaces. In that study, a 0.1 mg/mL solution of β-casein in Ca-free buffer resulted in a surface coverage of 650 ng/cm^2, and washing with protein-free buffer decreased the adsorbed layer to 430 ng/cm^2 (33). Although the magnitudes of adsorbed casein were different, the proportion of reversibly bound casein was similar to our results. A related study by Nylander et al. measured the adsorption of varying concentrations of β-casein to hydrophobic surfaces in Ca-free buffer (48). In 0.1 mg/mL β-casein (~4 μM), 250 ng/cm^2 of protein adsorbed, whereas at 0.01 mg/mL β-casein (~400 nM), ~220 ng/cm^2 adsorbed; after wash with protein-free solution, 200 ng/cm^2 remained in both cases. This reversibility is quantitatively consistent with the 500 nM K_D measured here for the reversible binding of soluble casein to the tightly bound casein monolayer (Fig. 3 and Table 1). Marchesseau et al. used surface plasmon resonance to measure the interactions between soluble casein subunits and subunits adsorbed to hydrophobic surfaces and measured affinities between 233 nM and 636 nM for α- and β-caseins, in good agreement with our results (31).

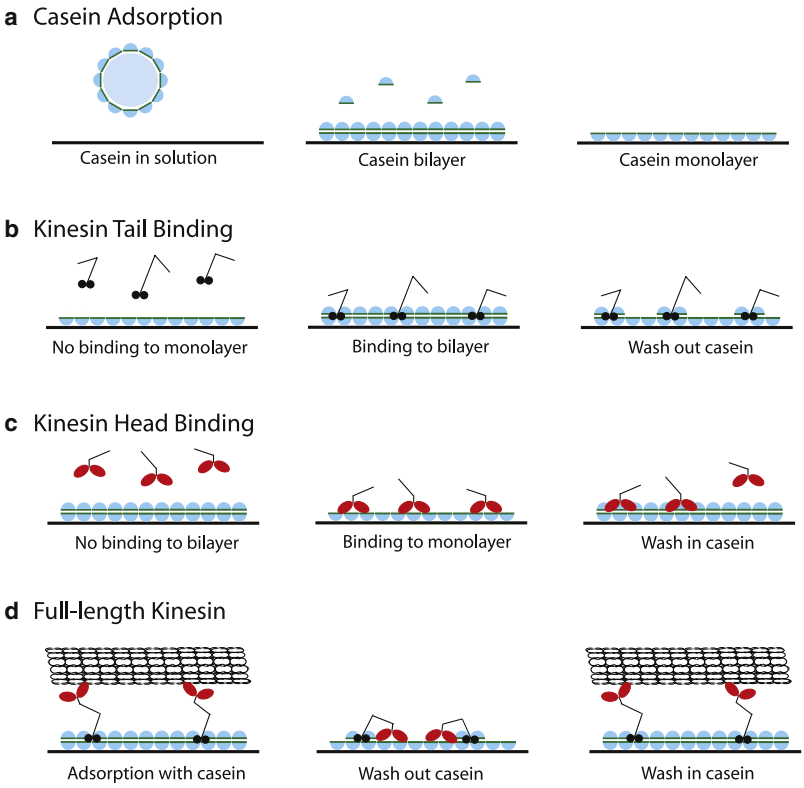

FIGURE 9 Proposed mechanism for the interaction of casein, kinesin, and microtubules with SiO_2 surfaces. (*a*) In solution, filtered casein exists as particles with mean diameter of 16 nm and, on interaction with the surface, dissociates into subunits that form a bilayer. Hydrophilic regions of the casein interact with the surface, and hydrophobic interactions stabilize interactions between the reversibly bound layer and the tightly bound layer. Removing the soluble casein results in dissociation of the reversibly bound casein, leaving a tightly bound monolayer on the surface. Note that the measured mass of the reversibly bound casein layer was only one-third of the tightly bound layer; however, for clarity here it is shown as a continuous layer. (*b*) In the absence of soluble casein, kinesin tails do not bind to the surface, but in the presence of soluble casein, the tails bind to the surface by interacting with both the tightly bound casein layer and the reversibly bound casein layer to form a tight interaction. Because of these stabilizing interactions, washing out soluble casein leaves both the tails and the associated subunits of reversibly bound casein on the surface. (*c*) In the presence of soluble casein, a casein bilayer blocks kinesin heads from interacting with the surface, but when soluble casein is removed, the heads bind to the tightly bound casein monolayer, presumably through hydrophobic interactions. This interaction is partially reversible, such that a wash step causes a portion of the heads to dissociate from the surface. (*d*) When adsorbed in the presence of soluble casein, kinesin binds to the surface through its tail domain, and the heads are free to interact with microtubules. Washing out the soluble casein results in the kinesin heads reversibly interacting with the tightly bound casein monolayer, such that reintroduction of soluble casein to form a bilayer rescues kinesin function.

We hypothesize that the forces associated with surface binding cause the 16-nm casein aggregates in solution to dissociate into their constituent subunits, which then bind tightly to the surface. The secondary, reversibly bound layer of casein can be understood by positing that the association forces governing reversible casein binding to the surface are the same intersubunit interactions that hold casein aggregates together in solution. One consequence of this model is that the solvent-exposed surfaces of adsorbed casein are expected to be quite different in protein-free solutions than in solutions where soluble casein is present and the reversibly bound secondary layer of casein can form. Our results support and extend a model put forward by Verma et al. (23), based on the amphipathic nature of casein (Fig. 9 *a*). If the hydrophilic regions of casein (presumably found on the exterior of casein submicelles) bind to glass and SiO_2 surfaces, exposing the hydrophobic regions of casein, then a surface that is pretreated with casein should have a hydrophobic character. Soluble casein will then reversibly interact with the exposed casein on the surface through hydrophobic interactions, resulting in a hydrophilic casein bilayer in the presence of soluble casein in solution. Differences in the binding of kinesin heads and tails to surfaces in the presence and absence of casein are interpreted below in the context of this casein bilayer model.

Kinesin heads and tails interact differently with casein-coated surfaces

Although soluble casein had little effect on the adsorption of full-length kinesin to casein-pretreated surfaces, truncated kinesins had strikingly different adsorption properties in the presence and absence of soluble casein: headless kinesin adsorbed well only in the presence of casein, whereas tailless kinesin adsorbed well only in the absence of soluble casein. Taken together with the finding of a reversibly bound casein layer, these results suggest that kinesin heads bind to the first casein layer but not to the second casein layer, whereas kinesin tails bind to the second casein layer but not to the first casein layer. However, this picture is clearly not complete, particularly with regard to the tail domain. If kinesin tails bind tightly to the second, reversibly bound casein layer, then washing out the reversibly bound casein should displace the tails from the surface. No such washout was observed in Fig. 6 *a*, excluding this simple model. Verma et al. (23) suggested a model in which kinesin tails bind to the tightly bound casein monolayer on the surface, but this model is unable to explain why binding of headless kinesin requires soluble casein in solution. A third model holds that even in the presence of bound casein on the surface, the kinesin tail binds directly to the surface (49). This model is simple,

and it is consistent with the ability of surface-adsorbed kinesin to withstand substantial mechanical forces. However, it does not explain why soluble casein (which if anything should block more of the surface) leads to enhanced kinesin tail binding.

A fourth model that does account for the tail-binding data is a cooperative model in which the kinesin tail interacts with both the tightly bound and the reversibly bound casein layers (Fig. 9 *b*). The paradigm for this type of cooperative binding model is the binding of dimeric lambda repressor protein to the operator site on lambda phage DNA, described in detail by Ptashne (50). Monomeric repressor subunits have a low affinity for DNA and a low affinity for one another, but if they are at a sufficiently high concentration to dimerize, then the interaction of the dimer with the operator DNA involves the summed free energies of interaction of the two subunits, resulting in a very high-affinity interaction. The observation that at a concentration of 3.7 nM headless kinesin, very little motor binds to the casein-coated surface in the absence of soluble casein (Fig. 5 *b*) puts a lower limit of ~100 nM for the K_D governing kinesin tail binding to the tightly bound casein on the surface. Positing a 1000-fold weaker association of the kinesin tail with soluble casein ($K_D = 100\ \mu M$) would mean that at the 9 μM (0.2 mg/mL) concentration of soluble casein used in the assays, >90% of the kinesin tail would be free and not bound to soluble casein in solution. From $\Delta G = RT \ln(K)$ (where $RT = 0.6$ kcal/mol and K is the equilibrium binding constant), the summed energies of kinesin binding to both the tightly and reversibly bound casein layers would be 15 kcal/mol, corresponding to a K_D of 10 pM. Although this approach ignores entropic effects, which will reduce the affinity, and the individual affinities may in fact be weaker than these estimates, this model is quantitatively consistent with the data. Furthermore, the fact that the kinesin tail is a stable dimer makes it reasonable to postulate that each tail domain is interacting with a different casein layer, or, if the two forms of casein interact with different regions of the tail domain, the dimerization could further contribute to this summed free energies effect.

Soluble casein enhances motor function by blocking the interaction of kinesin heads with the surface

In contrast to the behavior of the tail domain, kinesin heads were effectively prevented from adsorbing to the surface when the reversibly bound casein layer was present (Fig. 5 *c*). This result provides a general mechanism for how casein enhances motor activity: in the absence of casein the heads bind to the surface and inactivate, but in the presence of casein the heads do not bind, and only the tail binds (Fig. 9). If the solvent-exposed surface of the kinesin head contains a region of hydrophobic residues, then the energetics driving this surface binding can be explained by hydrophobic interactions between the head domains and the hydrophobic casein monolayer.

One question that is not easily resolved from the data is whether the interaction of the kinesin heads with the tightly bound casein monolayer is reversible. In the QCM experiment in Fig. 6 *b*, tailless kinesin adsorbed to the casein-treated surface in the absence of soluble casein, but washing in soluble casein to establish a hydrophilic casein bilayer did not displace the kinesin heads from the surface. In contrast, the functional assays in Fig. 8 suggest that inactivation of the kinesin heads (presumably through binding of the heads to the surface) is in fact reversible. In particular, Fig. 8 *a* shows that the activity of kinesin motors was enhanced to a greater degree by including soluble casein during the microtubule-binding step than during the motor adsorption step. Fig. 8 *b* shows that the reduction in motor activity resulting from removing soluble casein during the microtubule-gliding experiment can be reversed by washing soluble casein back into the flow cell. How can the QCM data and the microtubule binding data be resolved? The data are consistent with a model that includes both a reversible and a time-dependent irreversible interaction of kinesin heads with the tightly bound casein monolayer on the surface. For instance, in the QCM result in Fig. 6 *b*, which includes a 2-h adsorption step, washing out the free motors with casein-free buffer (point 5) does cause desorption of ~20% of the motors even though the subsequent introduction of soluble casein does not result in any more motors being washed off. This result suggests that in the QCM experiment a portion of the adsorbed motors are reversibly bound. Furthermore, the functional assays in Fig. 8 *b* show that, although washing soluble casein back into the flow cell does enhance motor activity, the microtubule landing rate does not return to the same level as before the casein washout. This result suggests that in the gliding assay a portion of the motors are irreversibly inactivated by removing the soluble casein.

A model that accounts for the bulk of the data is presented in Fig. 9 *d*. In the absence of weakly bound casein, the heads interact with the tightly bound casein monolayer, preventing them from binding to microtubules. This is consistent with the microtubule-binding data in Fig. 8 as well as with the observed casein dependence of tailless kinesin binding in Fig. 5. In contrast, in the presence of weakly bound casein, tail binding is favored, and the motor heads are prevented from interacting with the surface. This results in high microtubule-binding activity of the surface-adsorbed motors. The finding that this motor activity can be reversibly modulated by adding and removing casein suggests that kinesin head binding to the surface is reversible.

This model can explain two observations from the literature. Kim et al. found that in microtubule-gliding assays carried out using the standard casein protocol, 10–30-fold higher concentrations of tailless motors were required to match the microtubule-gliding activity of full-length kinesin

(51). The interpretation, based on our QCM experiments, is that in the presence of a casein bilayer, kinesins with no tail domain bind poorly to the surface and require much higher concentrations to achieve proper adsorption. In a different experiment, Huang et al. found that kinesin motors adsorbed to hydrophobic silane-treated surfaces in the presence of casein were completely inactive (12). The interpretation, based on our model of casein binding, is that casein adsorbs either poorly or in a different conformation on this hydrophobic surface, and the kinesin heads bind tightly to the hydrophobic surface and inactivate.

Although the model presented in Fig. 9 accounts for all of the experimental data in this study, the data cannot rule out the possibility that soluble casein enhances kinesin activity by acting as a chaperone and stabilizing the folding of the kinesin motor domain. Similar to many chaperone proteins, casein subunits are amphipathic, and a number of studies have found that α- and β-casein prevent aggregation of proteins such as alcohol dehydrogenase and insulin as well as or better than other classical chaperones (27,28). The presumed mechanism is that casein binds to hydrophobic regions of these proteins and prevents the hydrophobic interactions that lead to aggregation. If soluble casein subunits bound to kinesin and prevented inactivating head-tail or head-head interactions, this could lead to enhanced kinesin activity in the presence of soluble casein. However, despite reports of casein preventing protein aggregation, there are no reports of casein enhancing functional activity of proteins, and to become plausible this hypothesis requires considerable further experimentation.

CONCLUSIONS AND ONGOING QUESTIONS

Conventional kinesin serves as a model protein for understanding mechanochemistry at the molecular level, and it is hoped that uncovering the details of how kinesin binds to SiO_2 surfaces will provide a foundation for understanding the interaction of other motors and functional enzymes with engineered surfaces. These insights are important for developing functional assays and for developing future microscale devices such as sensors that incorporate biological components. Casein greatly enhances the functional activity of kinesin in microtubule-gliding assays. From QCM measurements, we demonstrate that casein binds to SiO_2 surfaces both as an irreversibly bound monolayer and as a reversibly bound second layer that has a magnitude one-third of the tightly bound layer and has a K_D of 500 nM. In the absence of this weakly bound casein layer, kinesin heads bind to the surface, but kinesin tails do not bind. In the presence of weakly bound casein, kinesin tails bind well to the surface, but kinesin heads do not bind and remain free to interact with microtubules. Because binding of the kinesin heads to the tightly bound casein monolayer is reversible, it is important to maintain casein in the solution to maximize the microtubule-binding activity of surface-adsorbed casein.

Although the data lead to a logical working model, a number of questions remain. What aspects of the motor heads and tails (charge, hydrophobicity, conformation, etc.) determine the interactions with casein-treated surfaces? Do the surfactant properties of casein underlie its function, and, if so, might other surfactants enhance motor activity to a similar or even greater degree? How can these findings be extended to novel motor proteins? Answering these questions should help the development of reliable design rules for engineering surfaces that maximize the activity of surface-bound proteins.

The authors thank Matthew Kutys for assistance running microtubule-gliding experiments and Shankar Shastry for protein purification work. Experiments were carried out while T.O. was a postdoctoral fellow in the laboratory of W.O.H. at Penn State University.

The work was supported by the National Science Foundation through the Penn State Center for Nanoscale Science (National Science Foundation MRSEC DMR0213623), by National Institutes of Health R01GM076476, and by ULVAC Inc. The authors declare no financial conflict of interest that would influence the results or interpretation of the experiments.

REFERENCES

1. Hancock, W. O. 2006. Protein-based nanotechnology: Kinesin-microtubule driven systems for bioanalytical applications. *In* Nanodevices for Life Sciences. C. Kumar, editor. Wiley-VCH, Weinheim, Germany. 241–271.
2. Hancock, W. O., and J. Howard. 1998. Processivity of the motor protein kinesin requires two heads. *J. Cell Biol.* 140:1395–1405.
3. Howard, J., A. J. Hudspeth, and R. D. Vale. 1989. Movement of microtubules by single kinesin molecules. *Nature*. 342:154–158.
4. Huang, Y.-M., M. Uppalapati, W. O. Hancock, and T. N. Jackson. 2007. Microtubule transport, concentration and alignment in enclosed microfluidic channels. *Biomed. Microdevices*. 9:175–184.
5. van den Heuvel, M. G., M. P. de Graaff, and C. Dekker. 2006. Molecular sorting by electrical steering of microtubules in kinesin-coated channels. *Science*. 312:910–914.
6. Berliner, E., H. K. Mahtani, S. Karki, L. F. Chu, J. E. Cronan, Jr., et al. 1994. Microtubule movement by a biotinated kinesin bound to streptavidin-coated surface. *J. Biol. Chem.* 269:8610–8615.
7. Valentine, M. T., P. M. Fordyce, T. C. Krzysiak, S. P. Gilbert, and S. M. Block. 2006. Individual dimers of the mitotic kinesin motor Eg5 step processively and support substantial loads in vitro. *Nat. Cell Biol.* 8:470–476.
8. Toyoshima, Y. Y., S. J. Kron, E. M. McNally, K. R. Niebling, C. Toyoshima, et al. 1987. Myosin subfragment-1 is sufficient to move actin filaments in vitro. *Nature*. 328:536–539.
9. Mehta, A. D., R. S. Rock, M. Rief, J. A. Spudich, M. S. Mooseker, et al. 1999. Myosin-V is a processive actin-based motor. *Nature*. 400:590–593.
10. Albet-Torres, N., J. O'Mahony, C. Charlton, M. Balaz, P. Lisboa, et al. 2007. Mode of heavy meromyosin adsorption and motor function correlated with surface hydrophobicity and charge. *Langmuir*. 23:11147–11156.
11. Månsson, A., M. Balaz, N. Albet-Torres, and K. J. Rosengren. 2008. In vitro assays of molecular motors–impact of motor-surface interactions. *Front. Biosci.* 13:5732–5754.
12. Huang, Y., M. Uppalapati, W. Hancock, and T. Jackson. 2005. Microfabricated capped channels for biomolecular motor-based transport. *IEEE T Adv Packaging*. 28:564–570.
13. Hirokawa, N., K. K. Pfister, H. Yorifuji, M. C. Wagner, S. T. Brady, et al. 1989. Submolecular domains of bovine brain kinesin identified

by electron microscopy and monoclonal antibody decoration. *Cell.* 56:867–878.

14. Yang, J. T., R. A. Laymon, and L. S. Goldstein. 1989. A three-domain structure of kinesin heavy chain revealed by DNA sequence and microtubule binding analyses. *Cell.* 56:879–889.
15. Kron, S. J., and J. A. Spudich. 1986. Fluorescent actin filaments move on myosin fixed to a glass surface. *Proc. Natl. Acad. Sci. USA.* 83:6272–6276.
16. Yanagida, T., M. Nakase, K. Nishiyama, and F. Oosawa. 1984. Direct observation of motion of single F-actin filaments in the presence of myosin. *Nature.* 307:58–60.
17. Howard, J., A. J. Hunt, and S. Baek. 1993. Assay of microtubule movement driven by single kinesin molecules. *Methods Cell Biol.* 39:137–147.
18. Block, S. M., L. S. Goldstein, and B. J. Schnapp. 1990. Bead movement by single kinesin molecules studied with optical tweezers. *Nature.* 348:348–352.
19. Romberg, L., and R. D. Vale. 1993. Chemomechanical cycle of kinesin differs from that of myosin. *Nature.* 361:168–170.
20. Ruettimann, K., and M. Ladisch. 1987. Casein micelles: structure, properties and enzymatic coagulation. *Enzyme Microb. Technol.* 9:578–589.
21. Phadungath, C. 2005. Casein micelle structure: a concise review. *Songklanakarin J. Sci. Technol.* 27:201–212.
22. Kerssemakers, J., J. Howard, H. Hess, and S. Diez. 2006. The distance that kinesin-1 holds its cargo from the microtubule surface measured by fluorescence interference contrast microscopy. *Proc. Natl. Acad. Sci. USA.* 103:15812–15817.
23. Verma, V., W. O. Hancock, and J. M. Catchmark. 2008. The role of casein in supporting the operation of surface bound kinesin. *J Biol Eng.* 2:14.
24. Swaisgood, H. E. 1993. Review and update of casein chemistry. *J. Dairy Sci.* 76:3054–3061.
25. McMahon, D. J., and W. R. McManus. 1998. Rethinking casein micelle structure using electron microscopy. *J. Dairy Sci.* 81:2985–2993.
26. Udabage, P., I. R. McKinnon, and M. A. Augustin. 2003. The use of sedimentation field flow fractionation and photon correlation spectroscopy in the characterization of casein micelles. *J. Dairy Res.* 70:453–459.
27. Bhattacharyya, J., and K. P. Das. 1999. Molecular chaperone-like properties of an unfolded protein, alpha(s)-casein. *J. Biol. Chem.* 274:15505–15509.
28. Wang, J. D., M. D. Michelitsch, and J. S. Weissman. 1998. GroEL-GroES-mediated protein folding requires an intact central cavity. *Proc. Natl. Acad. Sci. USA.* 95:12163–12168.
29. Morgan, P. E., T. M. Treweek, R. A. Lindner, W. E. Price, and J. A. Carver. 2005. Casein proteins as molecular chaperones. *J. Agric. Food Chem.* 53:2670–2683.
30. O'Connell, J. E., V. Y. Grinberg, and C. G. de Kruif. 2003. Association behavior of beta-casein. *J. Colloid Interface Sci.* 258:33–39.
31. Marchesseau, S., J. C. Mani, P. Martineau, F. Roquet, J. L. Cuq, et al. 2002. Casein interactions studied by the surface plasmon resonance technique. *J. Dairy Sci.* 85:2711–2721.
32. Fragneto, G., R. K. Thomas, A. R. Rennie, and J. Penfold. 1995. Neutron reflection study of bovine beta-casein adsorbed on OTS self-assembled monolayers. *Science.* 267:657–660.
33. Tiberg, F., T. Nylander, T. J. Su, J. R. Lu, and R. K. Thomas. 2001. β-Casein adsorption at the silicon oxide-aqueous solution interface. *Biomacromolecules.* 2:844–850.
34. Marx, K. A. 2003. Quartz crystal microbalance: a useful tool for studying thin polymer films and complex biomolecular systems at the solution-surface interface. *Biomacromolecules.* 4:1099–1120.
35. Matsuno, H., H. Faurusawa, and Y. Okahata. 2004. Kinetic study of phosphorylation-dependent complex formation between the kinase-inducible domain (KID) of CREB and the KIX domain of CBP on a quartz crystal microbalance. *Chem. Eur. J.* 10:6172–6178.
36. Coy, D. L., M. Wagenbach, and J. Howard. 1999. Kinesin takes one 8-nm step for each ATP that it hydrolyzes. *J. Biol. Chem.* 274:3667–3671.
37. Coy, D. L., W. O. Hancock, M. Wagenbach, and J. Howard. 1999. Kinesin's tail domain is an inhibitory regulator of the motor domain. *Nat. Cell Biol.* 1:288–292.
38. Hyman, A., D. Drechsel, D. Kellogg, S. Salser, K. Sawin, et al. 1991. Preparation of modified tubulins. *Methods Enzymol.* 196:478–485.
39. Williams, Jr., R. C., and J. C. Lee. 1982. Preparation of tubulin from brain. *Meth. Enzymol.,* 85 Pt. B:376–385.
40. Sauerbrey, G. 1959. Verwendung von Schwingquarzen zur Wagung dunner Schichten und zur Mikrowagun. *Z. Phys.* 155:206–222.
41. Böhm, K., R. Stracke, and E. Unger. 2000. Speeding up kinesin-driven microtubule gliding in vitro by variation of cofactor composition and physicochemical parameters. *Cell Biol. Int.* 24:335–341.
42. Ozeki, T., M. Morita, H. Yoshimine, H. Furusawa, and Y. Okahata. 2007. Hydration and energy dissipation measurements of biomolecules on a piezoelectric quartz oscillator by admittance analyses. *Anal. Chem.* 79:79–88.
43. Fischer, H., I. Polikarpov, and A. F. Craievich. 2004. Average protein density is a molecular-weight-dependent function. *Protein Sci.* 13:2825–2828.
44. Horne, D. S. 2006. Casein micelle structure: models and muddles. *Curr. Opin. Colloid Interface Sci.* 11:148–153.
45. Feder, J. 1980. Random sequential adsorption. *J. Theor. Biol.* 87:237–254.
46. Meyhofer, E., and J. Howard. 1995. The force generated by a single kinesin molecule against an elastic load. *Proc. Natl. Acad. Sci. USA.* 92:574–578.
47. Svoboda, K., C. F. Schmidt, B. J. Schnapp, and S. M. Block. 1993. Direct observation of kinesin stepping by optical trapping interferometry. *Nature.* 365:721–727.
48. Nylander, T., F. Tiberg, T. J. Su, J. R. Lu, and R. K. Thomas. 2001. β-Casein adsorption at the hydrophobized silicon oxide-aqueous solution interface and the effect of added electrolyte. *Biomacromolecules.* 2:278–287.
49. Fischer, T., and H. Hess. 2007. Materials chemistry challenges in the design of hybrid bionanodevices: supporting protein function within artificial environments. *J. Mater. Chem.* 17:943–951.
50. Ptashne, M. 1992. A Genetic Switch. Cell Press and Blackwell Science, Cambridge, MA.
51. Kim, T., M. T. Kao, E. F. Hasselbrink, and E. Meyhofer. 2007. Active alignment of microtubules with electric fields. *Nano Lett.* 7:211–217.
52. Eigler, W. N., J. N. Butler, C. A. Ernstrom, H. M. J. Farrell, V. R. Harwalkar, et al. 1984. Nomenclature of proteins of cow's milk, fifth revision. *J. Dairy Sci.* 67:1599–1631.